This manuscript is accepted to be published in Applied Mathematical Modelling

Transient air flow and heat transfer in a triangular enclosure with a conducting partition

Suvash C. Saha[1] Y. T. Gu[2]

School of Chemistry, Physics & Mechanical Engineering
Queensland University of Technology
2 George St., GPO Box 2434, Brisbane QLD 4001, Australia

Abstract

Numerical investigation is carried out for natural convection heat transfer in an isosceles triangular enclosure partitioned in the centre by a vertical wall with infinite conductivity. A sudden temperature difference between two zones of the enclosure has been imposed to trigger the natural convection. As a result, heat is transferred between both sides of the enclosure through the conducting vertical wall with natural convection boundary layers forming adjacent to the middle partition and two inclined surfaces. The Finite Volume based software, Ansys 14.5 (Fluent) is used for the numerical simulations. The numerical results are obtained for different values of aspect ratio, A (0.2, 0.5 and 1.0) and Rayleigh number, Ra ($10^5 \leq \mathrm{Ra} \leq 10^8$) for a fixed Prandtl number, Pr = 0.72 of air. It is anticipated from the numerical simulations that the coupled thermal boundary layers development adjacent to the partition undergoes several distinct stages including an initial stage, a transitional stage and a steady stage. Time dependent features of the coupled thermal boundary layers as well as the overall natural convection flow in the partitioned enclosure have been discussed in this study.

Keywords: Partition, natural convection, boundary layer, triangular enclosure, Nusselt number.

[1]Email: s_c_saha@yahoo.com, suvash.saha@qut.edu.au
[2]Corresponding author: YuanTong Gu, Email: yuantong.gu@qut.edu.au
Tel.:+61731381009 Fax: +61731381469

Nomenclature

A	aspect ratio
g	acceleration due to gravity
H	height of the enclosure
l	length of the enclosure
m	meter
N	number of partition
Nu_L	local Nusselt number
Nu	overall Nusselt number
p	pressure
Pr	Prandtl number
Ra	Rayleigh Number
s	second
t	time
t_s	steady state time scale
T	temperature of the fluid
T_c, T_h	temperatures of the cold and hot inclined walls
ΔT	temperature difference between the hot and cold inclined walls
u, v	velocity components in the x- and y- direction respectively
x, y	Cartesian coordinates

Greek letters

β	thermal expansion coefficient
δ_T	thickness of the thermal boundary layer
κ	thermal diffusivity
ρ	density of the fluid
ν	kinematic viscosity

1. Introduction

Natural convection occurs everywhere in nature. Natural convection in enclosures is a topic of considerable interest for the engineers. The main areas of studying natural convection are in the thermal design of buildings, solar collector design, nuclear reactor design, and others. Extensive studies of natural convection in the enclosures and adjacent to walls using analytical, experimental and numerical methods are available in the literature [1–4]. It

is noticeable that most of the studies devoted to an enclosure with no partitions. However, placing vertical partition in the enclosure can enhance or suppress heat transfer. There are several studies available in the literature related to vertical partition in the rectangular enclosure [5–11]. This problem is of fundamental importance for a variety of reasons. From the fundamental research point of view it is important to understand the interaction of two convective systems coupled across a partially conducting wall. The vertical conducting partition plays an important role in heat transfer between two fluid zones. It is seen from the earlier studies that the partition depresses natural convection in the cavity in comparison with that in a non-partitioned cavity for a laminar flow regime even though the partition is perfectly conducting [12–15].

Table 1: Previous partitioned cavity studies (rectangular cases)

Authors	Pr	Ra	N	A
Anderson and Bejan [16]	6	$10^9 \leq \mathrm{Ra} \leq 10^{10}$	0-2	0.33
Cuckovic-Dzodzo et al. [13]	2700-7000	$10^4 \leq \mathrm{Ra} \leq 10^6$	0-1	1.0
Nishimura et al. [15]	6	$10^8 \leq \mathrm{Ra} \leq 10^{10}$	0-4	4.0
Turkoglu and Yucel [18]	0.71	$10^5 \leq \mathrm{Ra} \leq 10^7$	0-4	0.5-1.5
Xu et al. [14]	7.0	1.8×10^9	0-1	1.0
Williamson et al. [26]	7.5	$0.6 - 1.6 \times 10^{10}$	0-1	1.0

Natural convection in rectangular enclosures with multiple vertical partitions is studied by [15–18] (see also in Table 1). The effect of multiple thin partitions has been investigated both experimentally and numerically by Nishimura et al. [15]. The experiments were performed in enclosures with aspect ratios, $A = 4$ and 10, for the range $10^6 \leq \mathrm{Ra} \leq 10^8$ and the range of partitions $1 \leq N \leq 4$. The authors concluded that the average Nusselt number is inversely proportional to $(1 + N)$. By placing double partitions in the middle of a rectangular enclosue, Anderson and Bejan [16] found that the heat transfer rate for double partitions is 20% less than that for a single partition. The similar studies were conducted by Jones [17] with multiple partitions for the case of laminar natural convection flows in rectangular enclosure. The author revealed that the effect of dividing the enclosure into six cells reduces the heat transfer rate by a factor of six.

In comparison with the rectangular or square enclosures, studies on triangular enclosure receive less attention before. However, because of its various

applications in many domestic and industrial systems as well as in geophysical flows, recently much attention is given to this geometry [19–24]. One of the important applications of studying this geometry is to investigate the fluid flow and heat transfer in the attic space. In both hot and cold climates the heat transfer through the attic space is seen as an important study for attic shaped houses. It is expected that one of the main objectives to design and construction of houses should be to provide thermal comfort for occupants. Moreover, it is also a requirement for houses to be energy efficient as the source of energy in the world is limited, i.e. the energy consumption for heating or air-conditioning houses must be minimized.

To control the heat transfer by placing a vertical partition into the triangular enclosure is still not available in the literature. The lack of such investigation has motivated the present study to investigate the heat transfer phenomena for partitioned triangular enclosure. The obtained results could help the builders for their insulation system in the attic shaped houses. The emphasis has been given to the transient process of natural convection resulting from a suddenly generated temperature difference between the fluids on the two sides of a conducting partition which has been placed along the geometric centre line of the enclosure. Effects of aspect ratio and Rayleigh number for heat transfer and fluid flow are also investigated in this study.

2. Problem formulation

Under consideration is an air filled triangular cavity of height H, half length of the base l, which is initially at quiescent. A partition is placed along the geometric centre line of the enclosure. Two interiors of both sides of the partition together with adjacent inclined walls receive different temperature with the left side receiving cold (T_c) and the right side receiving hot temperature (T_h) after time $t = 0s$. Two bottom tips of the enclosure are cut off by 5% to avoid singularities (see [19, 20, 22]) and rigid non-slip and adiabatic vertical walls are assumed at the cutting points (refer to Fig. 1). The bottom surface is also considered as adiabatic and rigid non-slip. The origin of the coordinate is the intersection point of the partition and the bottom surface.

The development of natural convection inside an attic space is governed by the following two-dimensional Navier-Stokes and energy equations with the Boussinesq approximation:

$$\frac{\partial u}{\partial x} + \frac{\partial v}{\partial y} = 0, \tag{1}$$

$$\frac{\partial u}{\partial t} + u\frac{\partial u}{\partial x} + v\frac{\partial u}{\partial y} = -\frac{1}{\rho}\frac{\partial p}{\partial x} + \nu\left(\frac{\partial^2 u}{\partial x^2} + \frac{\partial^2 u}{\partial y^2}\right), \tag{2}$$

$$\frac{\partial v}{\partial t} + u\frac{\partial v}{\partial x} + v\frac{\partial v}{\partial y} = -\frac{1}{\rho}\frac{\partial p}{\partial y} + \nu\left(\frac{\partial^2 v}{\partial x^2} + \frac{\partial^2 v}{\partial y^2}\right) + g\beta(T - T_0), \tag{3}$$

$$\frac{\partial T}{\partial t} + u\frac{\partial T}{\partial x} + v\frac{\partial T}{\partial y} = \kappa\left(\frac{\partial^2 T}{\partial x^2} + \frac{\partial^2 T}{\partial y^2}\right). \tag{4}$$

The three important parameters, which govern the natural convection, the Rayleigh number, the Prandtl number, and the aspect ratio are defined respectively as

$$\mathrm{Ra} = \frac{g\beta\Delta T H^3}{\kappa\nu}, \quad \mathrm{Pr} = \frac{\nu}{\kappa}, \quad \text{and} \quad A = \frac{H}{l}. \tag{5}$$

In this study the working fluid is considered as air ($\mathrm{Pr} = 0.72$); the range of aspect ratio of the enclosure as $0.2 \leq A \leq 1$ and the range of Rayleigh number as $10^5 \leq \mathrm{Ra} \leq 10^8$. The thickness of the partition is considered as zero with infinite conductivity, which is vertically placed in the geometric centreline of the enclosure and is diathermal for which only horizontal heat transfer is considered (refer to [8, 14, 16]) and all three surfaces and the partition are rigid and non-slip. The fluid inside the enclosure is initially at rest. At time $t = 0s$, the temperature of the fluid on the left side of the partition is $T = 290K$, and that on the right side of the partition is $T = 300K$.

3. Numerical scheme and grid and time step dependence tests

Equations (1) - (4) are solved along with the initial and boundary conditions using the SIMPLE scheme with the help of CFD software FLUENT 14.5. The finite volume method has been chosen to discretize the governing equations, with the QUICK scheme (see Leonard and Mokhtari [25]) approximating the advection term. The diffusion terms are discretized using central-differencing with second order accuracy. A second order implicit time-marching scheme has also been used for the unsteady term.

Two non-uniform grid sizes, 200×100 and 300×150 with coarser grids in the core and finer grids concentrated in the proximity of all wall and partition boundaries were constructed for grid dependence tests for $A = 0.5$. Fig. 2 plots time series of the temperatures at the point $P(-0.014m, 0.5m)$ of $A = 0.5$, in the middle of the thermal boundary layer on the left side of the partition calculated using the two grid systems for $\mathrm{Ra} = 10^8$. Clearly, two solutions almost overlapped. This means that either grid system is able to resolve the transient natural convection in the partitioned cavity and characterize the details of the boundary layers adjacent to the partition and other walls.

For time step dependency, two time steps of $0.05s$ (for 200×100 grid) and $0.01s$ (for 300×150 grid) are examined for $A = 0.5$. Fig. 2 shows the numerical results obtained using the above two time steps and their corrsponding grid sizes for $A = 0.5$. Evidently, the development of the flow is not sensitive to the two tested time steps, with either choice being satisfactory. Accordingly, the larger time step of $0.05s$ and coarser 200×100 grid are considered to be sufficiently small to capture the global transient features of the flow development and is adopted here for $A = 0.5$. The similar studies were conducted for two other aspect ratios. The similar grid size and time step of $A = 0.5$ is chosen for $A = 1.0$ and grid size of 400×100 and time step of $0.05s$ are chosen for $A = 0.2$ for the numerical simulations.

4. Results and discussions

4.1. Transient flow development

The time developments of the temperature at the point $(-0.014m, 0.5m)$ have been depicted in Fig. 2. This figure demonstrates the overall development of natural convection from a suddenly generated temperature difference between the fluids on the two sides of the partition to a steady state. As shown in Fig. 2, the flow development can be classified into three main stages: an initial stage, a transitional stage and a steady stage. At the early stage the conduction dominates the heat transfer. The temperature inside the boundary layer increases with time. When the conduction term in the energy equation balances with convection term, the scaling of that time (t_s) was given by Saha et al. [19, 20] as

$$t_s = \frac{(1 + \mathrm{Pr})^{0.5}}{\sin\theta(\mathrm{RaPr})^{0.5}} \left(\frac{H^2}{\kappa}\right) \tag{6}$$

where θ is the angle of the inclined surface with the horizontal. For the partition wall $\theta = \pi/2$. It is noted that the temperature growth does not cease immediately after t_s, time for convection to balance conduction. The flow undergoes several overshoots and undershoots during the transitional stage. As time progresses the thermal flows from the boundary layer of both sides of the partition discharge fluid into the core of the enclosure. At the end, the fluid inside the enclosure becomes steady state.

The time evolution of two isotherms ($T = 291K$ and $299K$) on both sides of the partition has been shown in Fig. 3. It is seen that the isotherms are shifting horizontally which means that the thickness of the coupled thermal boundary layers also increases with time. Saha et al. [19, 20] and others have pointed out that the thickness of the thermal boundary layer adjacent to an isothermal wall (either vertical or inclined) grows with time according to the scaling relation

$$\delta_T \sim \kappa^{0.5} t^{0.5} \tag{7}$$

Now, on the right side of the partition the cold fluid from the boundary layer has no choice but to travel down along the right horizontal intrusion. Eventually the fluid from the intrusion layer discharges into the core of the enclosure. On the other hand the hot fluid of the boundary layer of the left side of the partition moves up to the top tip and starts travelling along the left inclined wall. This fluid from the boundary layer also discharges into the core of the enclosure. At the end the fluid inside the enclosure becomes stratified. The steady state scaling value of the thermal layer thickness (Saha et al. [19, 20]) is,

$$\delta_{Ts} = \frac{H(1+\mathrm{Pr})^{0.25}}{\sin^{0.5}\theta(\mathrm{RaPr})^{0.25}} \tag{8}$$

4.2. Effect of aspect ratio

Steady state values of temperature contours and stream functions are depicted in Fig. 4 for three values of aspect ratio ($A = 0.2, 0.5$ and 1.0) while $\mathrm{Ra} = 10^8$. As it is seen in Fig. 4(a,c,e) the hot fluid from the thermal boundary layer adjacent to the left side of middle partition travels through the left inclined wall and discharges into the core region of the enclosure. The similar phenomena is seen on the right side of the partition. The cold fluid from the boundary layer travels downwards and then moves horizontally to the right. Gradually the whole enclosure becomes thermally stratified at the

steady stage for all three cases of aspect ratios. It is obseved that the flow becomes stronger when the aspect ratio is lower as it is evidenced by their stream function values.

Figure 5 shows the time developments of Nusselt number calculated on the middle partition for three different aspect ratios when $\mathrm{Ra} = 10^8$. Initially, the Nusselt number is very high for all aspect ratios as the heat transfer is dominated by conduction. Then the heat transfer decreaes sharply followed by a little oscillation in the transitinal stage. The Nusselt number then reduces gradually until it becomes completely steady state. It is revealed that the heat transfer strongly depends on the aspect ratio. The Nusselt number reduces as the aspect ratio increases.

4.3. Effect of Rayleigh number

Figure 6 shows the steady state values of temperature contours and streamlines for different values of Rayleigh number ($\mathrm{Ra} = 10^5, 10^6, 10^7$ and 10^8) while $A = 0.5$. It is observed in the isotherms that the fluid is horizontally stratified for higher Rayleigh number. For lower Rayleigh number the flow is weaker which is expected. The correspodning stream functions also confirm the flow is stronger for higher Rayleigh number. The flow is seen oscillating near the bottom surface when the Rayleigh number is higher. It is also noticed that the values of stream functions reduce when the Rayleigh number is reduced.

Time developments of Nusselt number on the middle partition has been shown in Fig. 7 for four different Rayleigh numbers when $A = 0.5$. Again, the Nusselt number is very high initially for all Rayleigh numbers as the heat transfer is dominated by pure conduction. However, the heat transfer is reduced dramatically with time after that and show a little oscillation as a form of undershoot and overshoot in the transitional stage. For higher Rayleigh number the Nusselt number reduces for some time and finally becomes steady state. However, the flow becomes steady state immidiately after the oscillation for lower Rayleigh numbers. This is because the flow is more stable for the lower Rayleigh number. It is also evident that the Nusselt number is very high for higher Rayleigh number because convection has a strong leading role for heat transfer.

Figure 8 shows the profiles of the local Nusselt numbers at the steady state on the partition and two inclined walls of the enclosure. It is clear that the local Nusselt number on the inclined walls is non-uniform and in the upstream section of the walls, it is much larger than that in the downstream

section due to the formation of the stratification in the core of the enclosure. However, the local Nusselt number on the partition is approximately constant but not so at two ends of the partition. The heat transfer through the middle height of partition does not vary with the height except for in the closeness to the top tip and the bottom wall. That means the partition is approximately isoflux at the steady state even though the inclined walls are isotherm which is an interesting phenomena at the steady state condition of the flow. Time series of the overall Nusselt number which are calculated on the inclined walls of the partitioned and non-partitioned triangular enclosure have been presented in Fig. 9. It is noticed that the Nusselt number on the left inclined cold wall (Fig. 9a) of the non-partitioned enclosure is higher at the transitional stage. However, the opposite scenario can be seen in the right heated wall (see Fig. 9b).

5. Conclusions

The coupled thermal boundary layers between the fluids of two zones in an isosceles triangular enclosure separated by a partition induced by suddenly generated temperature difference between the fluid zones are investigated numerically for different flow parameters. It is revealed that the development of the transient boundary layers adjacent to the partition are classified into three distinct stages; an initial stage, a transitional stage and a steady state stage. As soon as the fluids of two different temperatures reach the diathermal partition the coupled thermal boundary layers near both sides of the partition start to grow. When the conduction and convection terms in the energy equation are balanced the flow enters into the transitional stage. The thermal fluids discharged from the downstream ends of the coupled thermal boundary layers continuously fill each half of the partitioned cavity from transition stage to the steady state stage. As time progress another thermal boundary layer forms adjacent to the inclined wall. On a close observation of the flow phenomena in the transient process, it may be concluded that the temperature distribution on the partition enclosed by the coupled thermal boundary layers changes from an initially isothermal to an approximately linear profile at the steady state for higher Rayleigh number. As a result, an isoflux condition is set up along the middle portion of partition in the steady state stage. It is found from the numerical simulations that the heat transfer through the coupled thermal boundary layers is higher for lower aspect ratio for a fixed Rayleigh number. However, the heat transfer is higher for larger

Rayleigh number for a fixed aspect ratio.

References

[1] I. Catton, Natural convection in enclosures, Proc. 6th Int. Heat Transfer Conf., 6 (1978) 13 – 43.

[2] S. W. Churchill, Free convection in layers and enclosures. In Heat Exchanger Design Handbook, Chap. 2.5.8. Hemisphere, Washington, DC (1983).

[3] S.C. Saha, J.C. Patterson, C. Lei, Scaling of natural convection of an inclined flat plate: Ramp cooling condition, International Journal of Heat and Mass Transfer, 53, (2010) 5156 – 5166.

[4] S.C. Saha, R.J. Brown, Y.T. Gu, Prandtl number scaling of the unsteady natural convection boundary layer adjacent to a vertical flat plate for $Pr > 1$ subject to ramp surface heat flux, International Journal of Heat and Mass Transfer, 55 (2012) 7046 – 7055.

[5] H. Nakamura, Y. Asako, T. Hirata, Natural convection and thermal radiation in enclosures with a partition plate, Transaction of J.S.M.E. 850 (1984) 2647 – 2654.

[6] G.K. Bachelor, Heat transfer by free convection across a closed cavity between vertical boundaries at different temperatures, Quarterly of Applied Mathematics, 12 (1954) 209 – 233.

[7] E.R.G. Eckert, W.O. Carlson, Natural convection in an air layer enclosed between two vertical plates at different temperatures, International Journal of Heat and Mass Transfer, 2 (1961) 106 – 129.

[8] R. Anderson, A. Bejan, Natural convection on both sides of a vertical wall separating fluids at different temperature, ASME Journal of Heat Transfer, 102 (1980) 630 – 635.

[9] S. Acharya, C. H. Tsang. Natural convection in a fully partitioned. inclined enclosure, Numerical Heat Transfer - Part A, 8 (1985) 407 – 428.

[10] T. W. Tong, F. M. Gerner, Natural convection in partitioned air-filled rectangular enclosures. International Communications in Heat and Mass Transfer, 13 (1986) 99 – 108.

[11] T. Nishimura, M. Shiraishi, Y. Kawamura. Natural convection heat transfer in enclosures with an off-center partition, International Journal of Heat and Mass Transfer, 30 (1987) 1756 – 1758.

[12] D. Duxbury, An interferometric study of natural convection in enclosed plane air layers with complete and partial central vertical divisions, Ph.D. Thesis, University of Salford, (1979).

[13] D.M. Cuckovic-Dzodzo, M.B. Dzodzo, M.D. Pavlovic, Laminar natural convection in a fully partitioned enclosure containing fluid with nonlinear thermopysical properties, International Journal of Heat and Fluid Flow, 20 (1999) 614 – 623.

[14] F. Xu, J. C. Patterson, C. Lei, Heat transfer through coupled thermal boundary layers induced by a suddenly generated temperature difference, International Journal of Heat and Mass Transfer, 52 (2009) 4966 – 4975.

[15] T. Nishimura, M. Shiraishi, F. Nagasawa, Y. Kawamura, Natural convection heat transfer in enclosures with multiple vertical partitions, International Journal of Heat and Mass Transfer 31 (1988) 1679 – 1686.

[16] R. Anderson, A. Bejan, Heat transfer through single and double vertical walls in natural convection: theory and experiment, International Journal of Heat and Mass Transfer 24 (1981) 1611 – 1620.

[17] I. P. Jones, Numerical predictions from the IOTA 2 code for natural convection in vertical cavities, ASME Paper No. 82-HT-70 (1980).

[18] H. Turkoglu and N. Yucel, Natural convection heat transfer in enclosures with conducting multiple partitions and sidewalls. Heat Mass Transfer 32 (1996) 1 – 8.

[19] S.C. Saha, J.C. Patterson, C. Lei, Natural convection in attics subject to instantaneous and ramp cooling boundary conditions, Energy and Buildings 42 (2010) 1192 – 1204.

[20] S.C. Saha, J.C. Patterson, C. Lei, Natural convection in attic-shaped spaces subject to sudden and ramp heating boundary conditions, Heat and Mass Transfer 46 (2010) 621 – 638.

[21] S.C. Saha, J.C. Patterson, C. Lei, Natural convection and heat transfer in attics subject to periodic thermal forcing, International Journal of Thermal Sciences, 49 (2010) 1899 – 1910.

[22] S. C. Saha, Unsteady natural convection in a triangular enclosure under isothermal heating, Energy and Buildings, 43 (2011) 701 – 709.

[23] G.A. Holtzmann, R.W. Hill, K.S. Ball, Laminar natural convection in isosceles triangular enclosures heated from below and symmetrically cooled from above. ASME Journal of Heat Transfer, 122 (2000) 485 – 491.

[24] S. C. Saha, M. M. K. Khan, A review of natural convection and heat transfer in attic-shaped space, Energy and Buildings, 43 (2011) 2564 – 2571.

[25] B.P. Leonard, S. Mokhtari, ULTRA-SHARP Nonoscillatory Convection Schemes for High-speed Steady Multidimensional Flow, NASA TM 1e2568 (ICOMP-90-12). NASA Lewis Research Centre, 1990.

[26] N. Williamson, S. W. Armfield and M. P. Kirkpatrick, Transition to oscillatory flow in a differentially heated cavity with a conducting partition, Journal of Fluid Mechanics, 693 (2012) 93 – 114

Figure Captions:

Fig. 1. Schematic of the computational domains and boundary conditions.

Fig. 2. Time developments of the temperatures at the point $(-0.014m, 0.5m)$ in the middle of developed thermal boundary layer on the left side of the partition calculated using different meshes and time steps.

Fig. 3. Growth of the thermal boundary layers shown as isotherms for $T = 291K$ and $T = 299K$ at different times.

Fig. 4. Temperature contours (a, c, e) and stream functions (b, d, f) for different aspect ratio when Ra $= 10^8$.

Fig. 5. Temperature contours (a, c, e, g) and stream functions (b, d, f, h) for different values of Rayleigh number when $A = 0.5$.

Fig. 6. Time developments of Nusselt number through the vetical partition for different aspect ratio when Ra $= 10^8$.

Fig. 7. Time developments of Nusselt number through the vetical partition for different Rayleigh number when $A = 0.5$.

Fig. 8. Profiles of the local Nusselt numbers on the vertical partition and two inclined walls of enclosure.

Fig. 9. Time series of Nusselt number calculated on (a) left inclined walls , (b) right inclined walls of the partitioned and non-partitioned enclosure.

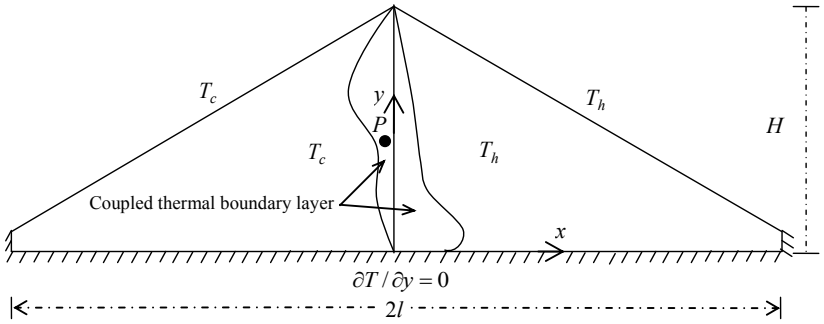

Figure 1: Schematic of the computational domains and boundary conditions.

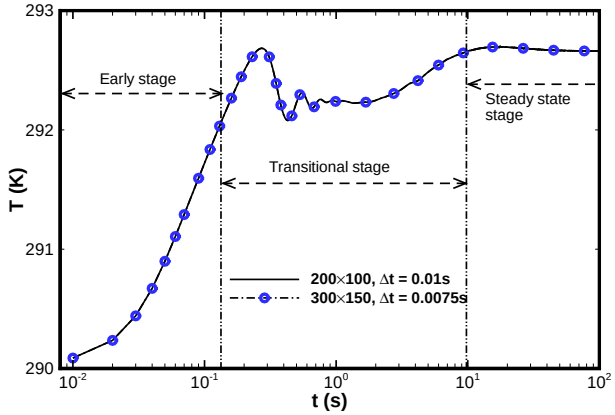

Figure 2: Time developments of the temperatures at the point $(-0.014m, 0.5m)$ in the middle of developed thermal boundary layer on the left side of the partition calculated using different meshes and time steps.

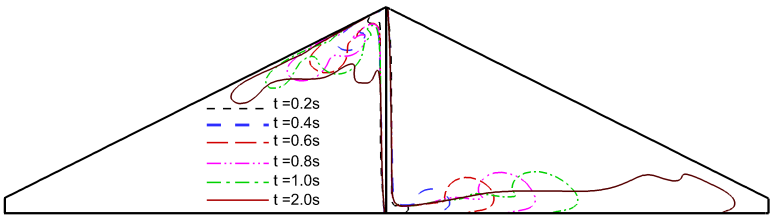

Figure 3: Growth of the thermal boundary layers shown as isotherms for $T = 291K$ and $T = 299K$ at different times.

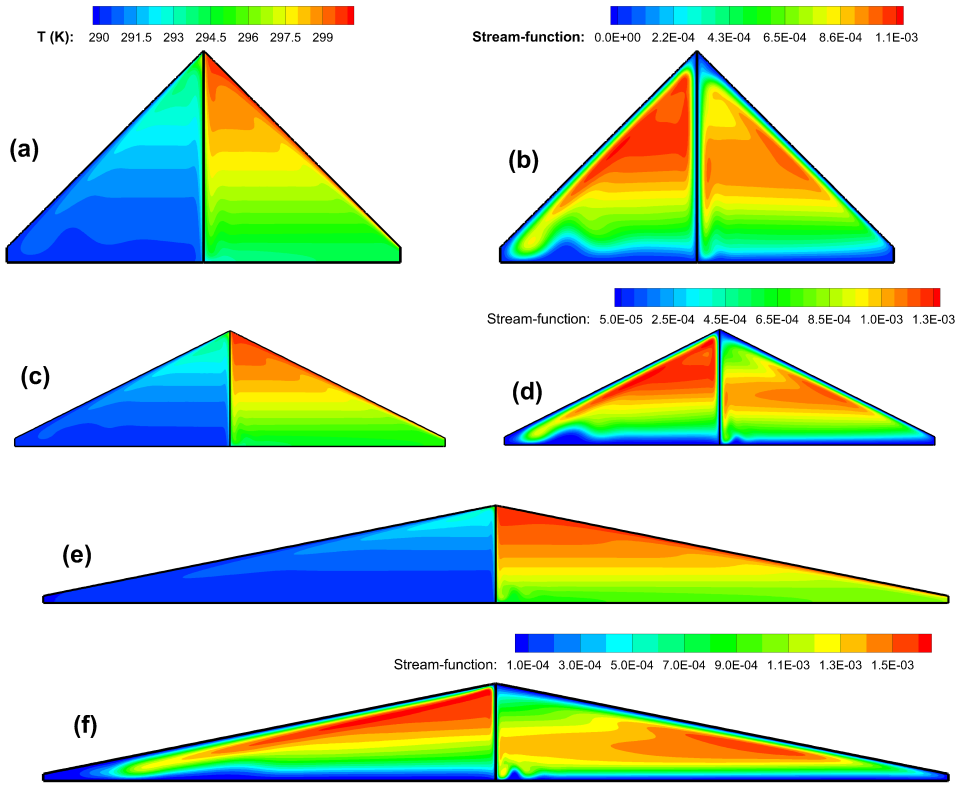

Figure 4: Temperature contours (a, c, e) and stream functions (b, d, f) for different aspect ratio when Ra = 10^8.

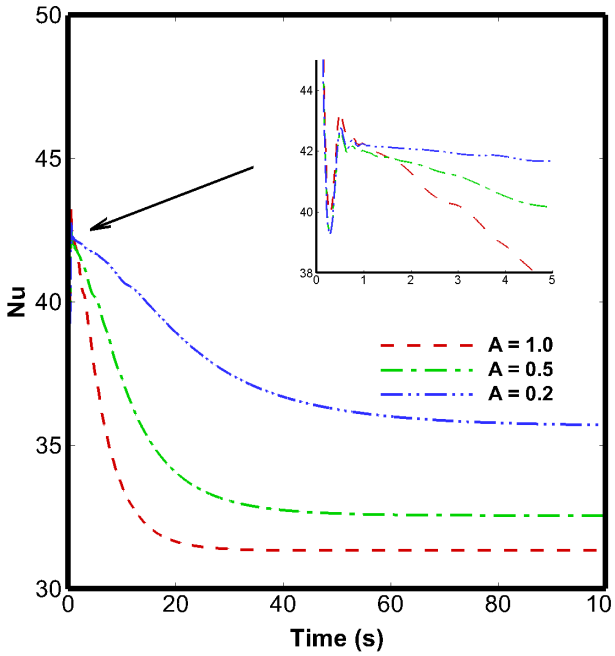

Figure 5: Time developments of Nusselt number through the vetical partition for different aspect ratio when Ra = 10^8.

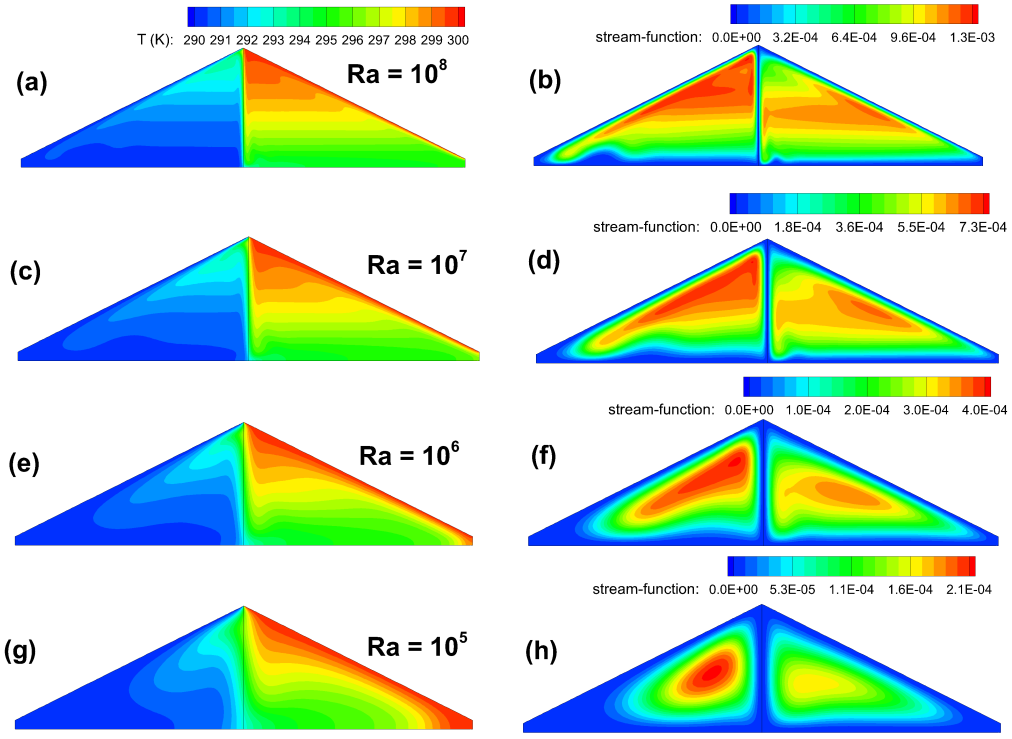

Figure 6: Temperature contours (a, c, e, g) and stream functions (b, d, f, h) for different values of Rayleigh number when $A = 0.5$.

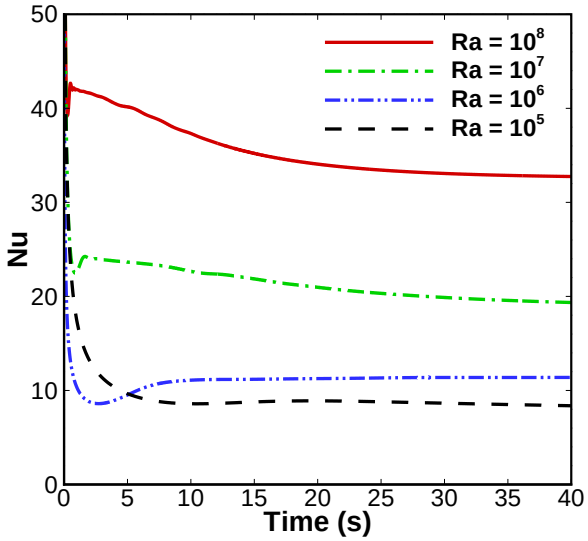

Figure 7: Time developments of Nusselt number through the vetical partition of the emclosure for different Rayleigh number when $A = 0.5$.

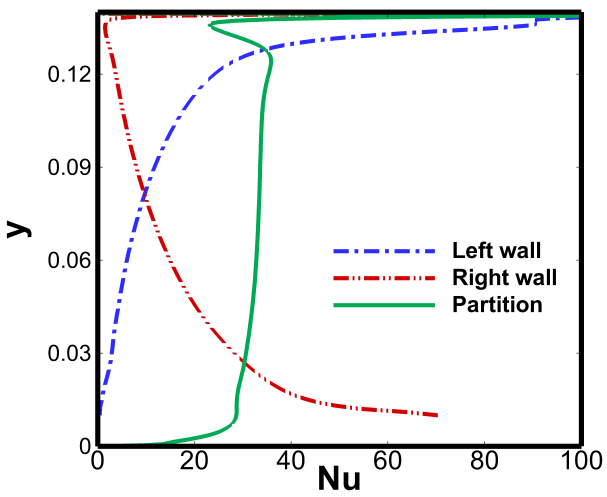

Figure 8: Profiles of the local Nusselt numbers on the vertical partition and two inclined walls of enclosure.

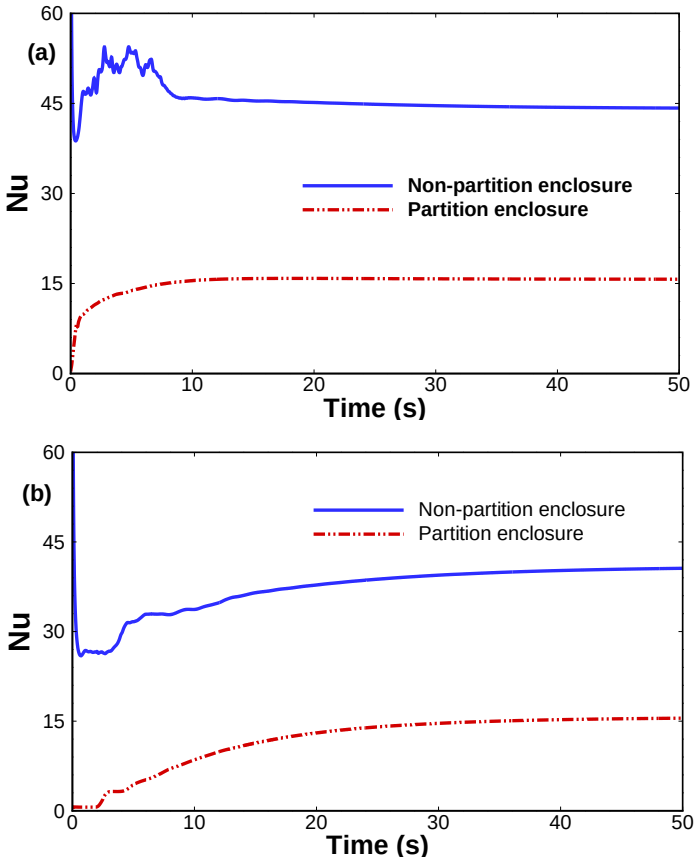

Figure 9: Time series of Nusselt number calculated on (a) left inclined walls , (b) right inclined walls of the partitioned and non-partitioned enclosure.